A 3.5/5.9-GHz Dual-Band Output Matching Network for an Efficiency-Optimized Multiband Power Amplifier

Allison Duh, Sushia Rahimizadeh, Taylor Barton, Zoya Popović
University of Colorado at Boulder

Abstract — This paper describes the design and implementation of a dual-band output matching network (OMN) to enable the design of a dual-band power amplifier. The three-port network transforms 50-Ω loads and presents, in two separate bands around 3.5 and 5.9 GHz, optimized fundamental impedances to a GaN HEMT transistor for maximum power added efficiency (PAE). The OMN is comprised of four subcircuits: two circuits perform a real-to-real impedance transformation and two perform a real-to-complex impedance transformation, connected to the transistor through a tee junction. The measured performance of the passive networks shows high isolation between the bands.

Index Terms — Dual band, impedance matching, microwave amplifiers

I. INTRODUCTION

Multi-carrier and carrier aggregation schemes are increasingly used in communications systems to improve data rates and spectral efficiency. As a result, there has recently been significant interest in power amplifiers (PAs) able to operate over multiple bands, whether through broadband [1], multi-band [2], or frequency-reconfigurable techniques [3]. In each of these approaches, the output matching network (OMN) presents a major design challenge, as the frequency-dependent target loading impedances for the active device tend to exhibit a non-Foster rotation in the Smith chart.

A simple approach to amplify widely disparate carrier frequencies is to employ two narrowband PAs, each designed for one carrier frequency, with a wideband power combining network or diplexer. A drawback of this architecture is that the active devices may be underutilized if only one carrier frequency is used, or if the signals at different frequencies have different power levels. Another option is the co-design of amplifier and matching network, as demonstrated in [1][4], where the two are designed in an integrated fashion to reduce insertion loss and mismatch, thus increasing efficiency and bandwidth.

Recent dual-band PA design covers a wide swath of frequency bands and technologies. [5] focuses on lower frequency bands (800 MHz/2.4 GHz) with an emphasis in low-complexity and drain efficiency 53.9% and 41.3%, respectively. [6] presents a dual-band matching network with an incorporated dual-band filter for 800 MHz and 1.9 GHz, with PAE>65% from a 45-W GaN device.

Another work, [7], operates at higher frequencies of 3.1 and 8.0 GHz, and yields 24.3/21.2 dBm of output power with peak drain efficiency of 34.8% and 12.2%, respectively.

In this work, we propose an alternative approach to a multi-frequency transmitter in which a single PA drives two loads (antennas) in different bands. A three-port OMN is designed with the dual functions of presenting the (frequency-dependent) desired load impedance to the device at both bands, and acting as a diplexer in that the output power goes to the desired load. A block diagram of the architecture is shown in Fig. 1. This paper describes a design approach to the three-port OMN and gives a design example for a 6-W GaN packaged device operating in the 3.5-GHz and 5.9-GHz bands.

II. DESIGN METHODOLOGY

The OMN consists of four subcircuits in two branches. Using the load as a reference plane and moving back towards the transistor drain, each branch has a subcircuit which transforms the 50-Ω load to two intermediate real impedances at the two design frequencies, ($R_{LP,3.5}$ and $R_{LP,5.9}$). This real-to-real (R-R) transformation is followed by two subcircuits which perform real-to-complex (R-C) impedance transformations in order to present the load-pull complex impedances at the drain of the device ($Z_{LP,3.5}$ and $Z_{LP,5.9}$). The transistor and the branches of the OMN are connected through a tee junction; each branch is designed such that it presents the target impedance within their band, but acts as an effective open to the other band. This prevents each branch from loading the other, and thus also prevents signal transmission outside of the design frequencies of the two bands.

A Wolfspeed (Cree) 6-W CGH40006P packaged device is used for the design example and prototype. Load-pull simulations are performed at two frequencies, 3.5 GHz and 5.9 GHz, using Keysight ADS with the manufacturer-provided nonlinear transistor model. The device is biased in deep AB mode, with $V_{DS} = 28$ V and $I_{DS} = 40.8$ mA. A stability circuit is designed at the gate and consists of a parallel RC (ATC600S 2-pF, KOA0402 50-Ω). Simulated load pull contours at the two design frequencies are shown in Fig. 2. The point of optimal PAE
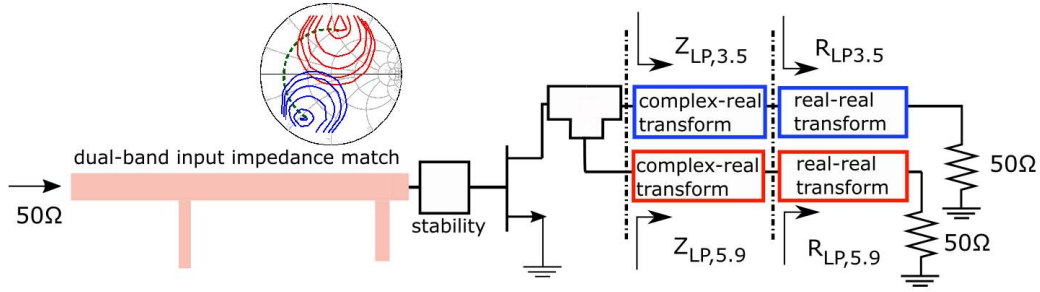
Fig. 1. Block diagram of the dual-band dual-load PA. The dual-band input matching network is designed from simulated source-pull and includes an RC stability network. The output network is the focus of this paper and consists of two R-C impedance transformers and two R-R sixth-order Chebyshev transformers.

is centered at $14.4 + j2.7\,\Omega$, at 3.5 GHz, and at $26.8\text{-}j62\,\Omega$ at 5.9 GHz. As 5.9 GHz approaches the upper limit of this transistor's frequency range, the input drive is 28 dBm, 2 dB more than at the lower band.

Given the load-pull contours, the R-R impedance transforming networks are designed to match $50\,\Omega$ to $10\,\Omega$ and $25\,\Omega$, respectively, with the S-band path designed as a low-pass filter and the C-band path as a high-pass filter. Sixth-order Chebyshev lumped networks are used, following tables in [8]. After converting the lumped element values to transmission lines such that the impedance transformation is preserved in the band of interest, the circuits are tuned to present a high impedance out of band to reflect undesired power. In the case of the 3.5-GHz R-R subcircuit, this involves a length of line and a stub on the input side of the circuit; for the 5.9 GHz R-R subcircuit, a $70\text{-}\Omega$ line of 178 electrical degrees at 5.9 GHz is sufficient. The R-R impedance transformation circuits are EM simulated with ADS Momentum to ensure accuracy after fabrication.

Various topologies were investigated for the design of the R-C subcircuits, with low insertion loss and small footprint as design goals. A stub-tuned design was chosen for both R-C subcircuits, to increase the ability of the network to present resonant loops, and optimized with lumped element capacitors to minimize circuit size.

III. IMPLEMENTATION AND PERFORMANCE

The OMN is fabricated on a 30-mil, 0.5 oz-clad Rogers 4350B substrate (Fig. 4). Because the input plane of the three-port is designed to be at the tee, a $50\text{-}\Omega$ line runs from the tee to Port 1 and is de-embedded in subsequent measurements. 4-mm long $50\text{-}\Omega$ lines are also milled to offset the length of SMA connectors from the termination of each output port. The lumped components used in the circuit are three ATC600S capacitors (3.9, 11, 18 pF). As shown in Fig. 3, the three-port correctly presents the
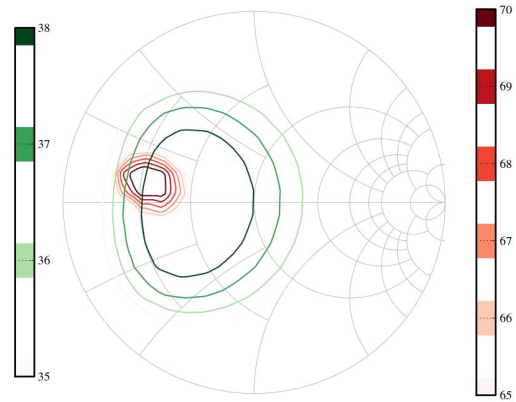
(a) 3.5-GHz contours for PAE (red, legend right) and power delivered in dBm (green, legend left)
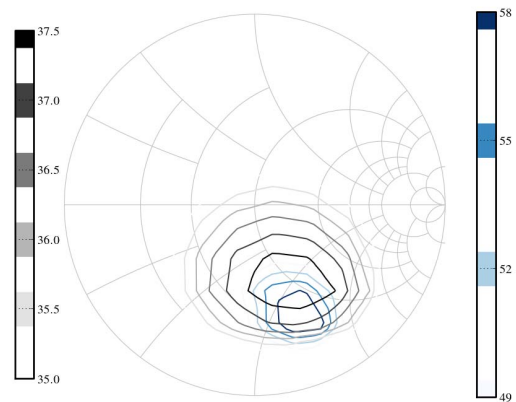
(b) 5.9-GHz contours for PAE (blue, legend right) and power delivered in dBm (gray, legend left)

Fig. 2. Simulated load pull contours of the 6-W device at the two frequency bands of interest.
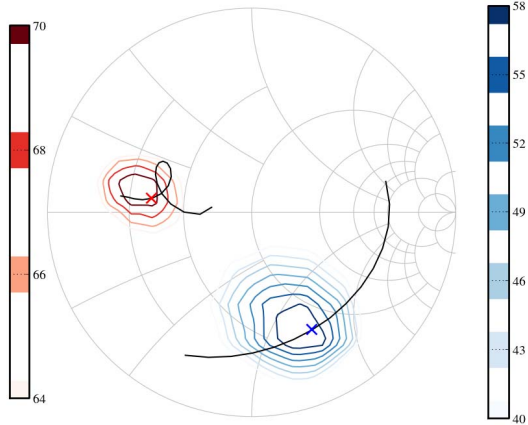
Fig. 3. Simulated load-pull contours for PAE are plotted for 3.5 (red) and 5.9 GHz (blue) bands, respectively. The input reflection ($|S_{11}|$ parameter) of the fabricated circuit is plotted across the two frequency bands of interest, with the response at 3.5 and 5.9 GHz marked accordingly.
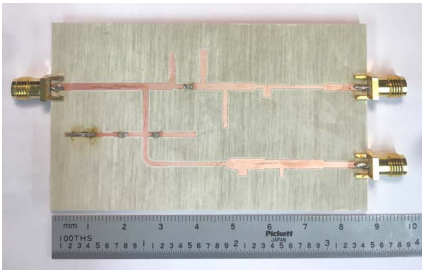

Fig. 4. Photo of the fabricated circuit, with upper branch connected to the 3.5, and the lower to the 5.9 GHz load.

Fig. 5. Measured and simulated insertion loss (top) and return loss (bottom) over frequency, assuming 50-Ω and transistor complex impedance at the two ports (Fig.1).

TABLE I
PREDICTED POWER AMPLIFIER PERFORMANCE

Frequency (GHz)	PAE (%)	Power delivered (dBm)
3.5	45.9	37.2
5.9	32	34.6

desired impedances in both bands. In calculating the return and insertion losses, the input port impedance is set to the conjugate impedance of the target impedances described in Section II, $Z_{LP,3.5}$ and $Z_{LP,5.9}$. The return loss is measured to be 14.8 dB for the 3.5 GHz band, 21.3 dB in the 5.9 GHz band, compared with simulated results of 16.9 dB and 8.6 dB. The frequency shift in the upper band is likely due to fabrication error and can be mitigated with more exact circuit-printing methods. Insertion loss is here defined as dissipative loss due to attenuation, and takes into account the effect of matching to a non-50Ω impedance, as $IL = 10 \cdot log_{10}(|S_{21}|^2/(1 - |S_{11}|^2))$. The measured three-port prototype demonstrates 1.2 and 2.46 dB of insertion loss at 3.5 and 5.9 GHz, respectively.

IV. CONCLUSION

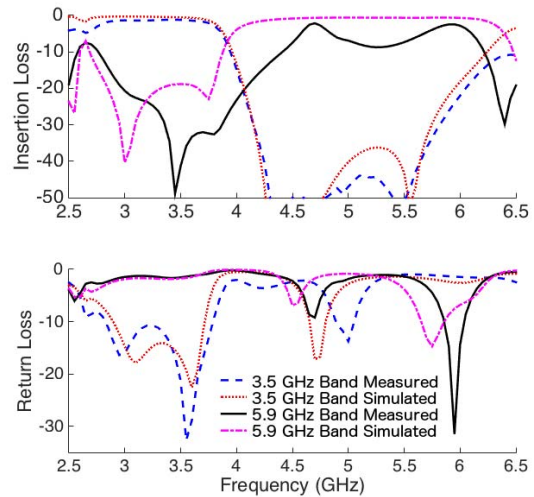This paper presents a design approach for the output network of a dual-band dual-load high-efficiency PA with bands at 3.5 and 5.9 GHz, designed to have frequency-selective characteristics and match to the complex load-pulled optimal impedance of the device. With the measured results for the passive matching networks, the predicted PAE and output power of the PA is shown in Table I. The insertion loss of the lower band remains constant from approximately 3 to 4 GHz, indicating strong potential for the OMN to cover an octave bandwidth between the two bands. The reduced efficiency at 5.9 GHz is due to the increased insertion loss in the higher frequency band and degradation of device performance range at a higher frequency; an improved version will be implemented in ongoing work on a complete power amplifier incorporating the dual-band network.

REFERENCES

[1] K. Chen and D. Peroulis, "Design of Adaptive Highly Efficient GaN Power Amplifier for Octave-Bandwidth

Application and Dynamic Load Modulation," *IEEE Transactions on Microwave Theory and Techniques*, vol. 60, no. 6, pp. 1829–1839, 2012.

[2] K. Chen, E. J. Naglich, Y. C. Wu, and D. Peroulis, "Highly linear and highly efficient dual-carrier power amplifier based on low-loss RF carrier combiner," *IEEE Trans. Microw. Theory Techn.*, vol. 62, no. 3, pp. 590–599, March 2014.

[3] H. M. Nemati, J. Grahn, and C. Fager, "Band-Reconfigurable LDMOS Power Amplifier," *40th European Microwave Conference*, no. September, pp. 978–981, 2010.

[4] Y. C. Li, K. C. Wu, and Q. Xue, "Power Amplifier Integrated With Bandpass Filter for Long Term Evolution Application," vol. 23, no. 8, pp. 424–426, 2013.

[5] J. H. Mueller, M. Scholl, Y. Zhang, L. Liao, A. Atac, Z. Chen, B. Mohr, R. Wunderlich, and S. Heinen, "A Low Complexity Multistandard Dual Band Wireless Transceiver with Integrated 24 . 7 dBm 54 % Efficiency Polar PA in a 0 . 13 μm CMOS Technology," pp. 52–54, 2017.

[6] X. Fu, D. T. Bespalko, and S. Boumaiza, "Novel dual-band matching network for effective design of concurrent dual-band power amplifiers," *IEEE Transactions on Circuits and Systems I: Regular Papers*, vol. 61, no. 1, pp. 293–301, Jan 2014.

[7] J. Ko, S. Lee, and S. Nam, "An S / X-Band CMOS Power Amplifier Using a Transformer-Based Reconfigurable Output Matching Network," vol. 1, pp. 344–347, 2017.

[8] G. L. Matthaei, "Tables of Chebyshev impedance-transforming networks of low-pass filter form," *Proc. IEEE*, vol. 52, no. 8, pp. 939–963, Aug 1964.